Optical ventricular cardioversion by local optogenetic targeting and LED implantation in a cardiomyopathic rat model

Nyns, Emile C.A.; Jin, Tianyi; Fontes, Magda S.; van den Heuvel, Titus; Portero, Vincent; Bart, Cindy I.; Zeppenfeld, Katja; Zhang, Guoqi; Poelma, René H.; More Authors

DOI
10.1093/cvr/cvab294

Publication date
2022

Document Version
Final published version

Published in
Cardiovascular research

Citation (APA)
Nyns, E. C. A., Jin, T., Fontes, M. S., van den Heuvel, T., Portero, V., Bart, C. I., Zeppenfeld, K., Zhang, G., Poelma, R. H., & More Authors (2022). Optical ventricular cardioversion by local optogenetic targeting and LED implantation in a cardiomyopathic rat model. *Cardiovascular research*, *118*(10), 2293-2303. https://doi.org/10.1093/cvr/cvab294

ESC European Society of Cardiology

Cardiovascular Research (2022) **118**, 2293–2303
https://doi.org/10.1093/cvr/cvab294

Optical ventricular cardioversion by local optogenetic targeting and LED implantation in a cardiomyopathic rat model

Emile C.A. Nyns[1], Tianyi Jin [2†], Magda S. Fontes[1†], Titus van den Heuvel[1], Vincent Portero [1], Catilin Ramsey[2], Cindy I. Bart[1], Katja Zeppenfeld [1], Martin J. Schalij[1], Thomas J. van Brakel [3], Arti. A. Ramkisoensing[1], Guoqi Zhang[2], René H. Poelma [2], Balazs Ördög[1], Antoine A.F. de Vries [1†], and Daniël A. Pijnappels [1*†]

[1]Laboratory of Experimental Cardiology, Department of Cardiology, Leiden University Medical Center (LUMC), Albinusdreef 2, 2300 RC, Leiden, The Netherlands; [2]Department of Microelectronics, Delft University of Technology, Mekelweg 4, 2628 CD, Delft, The Netherlands; and [3]Department of Cardiothoracic Surgery, LUMC, Albinusdreef 2, 2300 RC, Leiden, The Netherlands

Received 30 December 2020; editorial decision 3 September 2021; accepted 9 September 2021; online publish-ahead-of-print 16 September 2021

Time for primary review: 40 days.

Aims Ventricular tachyarrhythmias (VTs) are common in the pathologically remodelled heart. These arrhythmias can be lethal, necessitating acute treatment like electrical cardioversion to restore normal rhythm. Recently, it has been proposed that cardioversion may also be realized via optically controlled generation of bioelectricity by the arrhythmic heart itself through optogenetics and therefore without the need of traumatizing high-voltage shocks. However, crucial mechanistic and translational aspects of this strategy have remained largely unaddressed. Therefore, we investigated optogenetic termination of VTs (i) in the pathologically remodelled heart using an (ii) implantable multi-LED device for (iii) *in vivo* closed-chest, local illumination.

Methods and results In order to mimic a clinically relevant sequence of events, transverse aortic constriction (TAC) was applied to adult male Wistar rats before optogenetic modification. This modification took place 3 weeks later by intravenous delivery of adeno-associated virus vectors encoding red-activatable channelrhodopsin or Citrine for control experiments. At 8–10 weeks after TAC, VTs were induced *ex vivo* and *in vivo*, followed by programmed local illumination of the ventricular apex by a custom-made implanted multi-LED device. This resulted in effective and repetitive VT termination in the remodelled adult rat heart after optogenetic modification, leading to sustained restoration of sinus rhythm in the intact animal. Mechanistically, studies on the single cell and tissue level revealed collectively that, despite the cardiac remodelling, there were no significant differences in bioelectricity generation and subsequent transmembrane voltage responses between diseased and control animals, thereby providing insight into the observed robustness of optogenetic VT termination.

Conclusion Our results show that implant-based optical cardioversion of VTs is feasible in the pathologically remodelled heart *in vivo* after local optogenetic targeting because of preserved optical control over bioelectricity generation. These findings add novel mechanistic and translational insight into optical ventricular cardioversion.

Keywords Optogenetics • Ventricular tachycardias • Remodelling • *In vivo*

*Corresponding author. Tel: + 31 71 5265330; fax: +31 71 526 68 09, E-mail: d.a.pijnappels@lumc.nl
†These authors contributed equally to the study.

1. Introduction

Biological excitation (i.e. generation of bioelectricity) plays a key role in the functioning of various organs, including the brain and heart. For the heart, disturbances in this process could lead to rhythm disorders including ventricular tachycardias (VTs), which are an important source of morbidity and sudden cardiac death worldwide.[1,2] VTs most often occur in the setting of structural heart disease, i.e. in the pathologically remodelled heart.[3] Current therapies for VTs include anti-arrhythmic drugs, catheter ablations, and implantable cardioverter defibrillators (ICDs). While drug treatment is often ineffective and hampered by side effects, catheter ablation can be effective for a selected subgroup of patients with monomorphic VTs and accessible substrates. However, catheter ablation may result in irreversible complications and generally comes with modest long-term efficacy. In contrast, high-voltage shocks from ICDs do terminate VTs in an effective manner and have been proven to reduce mortality in different cohorts of patients. These shocks are, however, not only very painful and can lead to depression and anxiety, but may also be delivered inappropriately and cause cardiac tissue damage.[4,5] The development of novel therapies that decrease such adverse effects, while improving the termination success of hazardous VTs is hence of enduring relevance.

Optogenetics is a novel technology by which selected cells can be controlled in various ways and with an unprecedented degree of spatiotemporal control after being modified to express light-sensitive proteins.[6] One class of such proteins are the channelrhodopsins, non-selective cation channels that open upon exposure to light of specific wavelengths. Illumination of channelrhodopsin-expressing cardiomyocytes results in sustained depolarization of the sarcolemma for the duration of illumination. Such optically controlled generation of bioelectricity has recently been applied in healthy rodents to pace the heart and to terminate pharmacologically induced arrhythmias, including VTs in *ex vivo* studies of isolated, non-remodelled hearts subjected to global and patterned illumination of the epicardium by an external light source.[7–12] VTs, however, typically occur in pathologically remodelled hearts, while for their optogenetic termination to be realized in a clinically more relevant setting, an implantable light source for closed-chest, local illumination would be required.

In order to explore these translational requirements of optogenetic VT termination, we used adult rats selectively expressing the light-gated ion channel red-activatable channelrhodopsin (ReaChR) in cardiomyocytes. In these rats, the pathological structural and electrophysiological changes that are so prevalent among VT patients were mimicked using transverse aortic constriction (TAC)-induced chronic pressure overload resulting in a cardiomyopathic phenotype characterized by myocardial hypertrophy and fibrosis. Moreover, we refined the illumination method by applying a custom-made, implantable LED device for local illumination of the apex of the heart to enable experiments in the fully closed-chest *in vivo* setting.

2. Methods

A detailed description of all methods and materials is provided in the Supplementary material online.

2.1 Study design

All animal experiments were approved by Animal Experiments Committee of the Leiden University Medical Center, the Netherlands (AVD1160020172929) and performed in accordance with the guidelines from Directive 2010/63/EU of the European Parliament on the protection of animals used for scientific purposes. The experimental design of the study is illustrated in *Figure 1A*. At indicated timepoints post-TAC or sham surgery, male Wistar rats (Crl: WI[WU]; Charles River Laboratories, Cologne, Germany) were subjected to electro- and echocardiographic measurements and received adeno-associated virus vectors (AAVVs) (2×10^{13} genome copies) coding for ReaChR, or Citrine as negative control protein. Male rats were used because their hearts are larger than those of age-matched female rats, which facilitated the induction of sustained VTs. The feasibility and efficacy of optical VT termination were assessed by *ex vivo* and *in vivo* apical illumination of the heart. To this purpose, a miniaturized device was constructed that consisted of four LEDs producing 567 nm (lime) or 617 nm (red) light (LUXEON Z Color line LXZ1, Lumileds, San Jose, CA), a support frame, and a transparent layer of UV curable optical adhesive (NOA63, Norland Products, Cranbury, NJ). Electrophysiological, histological, and optical studies were performed at the cellular and/or tissue level for safety assessment and in-depth mechanistic insight.

2.2 TAC surgery and intravenous AAVV injections

Rats were anaesthetized using 2–3% isoflurane vapour in O_2 at 0.8 L/min. Baseline ECG data were collected using an 8-channel PowerLab data acquisition device and recorded and analysed using LabChart Pro software version 7 (both from ADInstruments, Oxford, UK). The rats were 9–10 weeks old when they underwent TAC or sham surgery. Adequate anaesthesia was confirmed by the absence of the pedal reflex. Pressure overload was induced via TAC surgery as previously described.[13] Briefly, the aorta was exposed via the second left intercostal space. A 4-0 silk suture was placed around the aorta between the brachiocephalic trunk and left common carotid artery. A spacer made from a 21 G hypodermic needle was placed next to the transverse aorta. To constrict the aorta, the suture was tied around the aorta and spacer before removing the spacer. Animals assigned to receive sham surgery underwent the same procedure, except that no suture was tied around the aorta. Adequate analgesia was provided before and after surgery by subcutaneous injections of buprenorphine hydrochloride (0.05 mg/kg). In the first 3 days following surgery, subcutaneous injections were administered twice a day in case of signs of discomfort. Three weeks after successful TAC or sham surgery, 2×10^{13} genome copies of AAV2/9.45.GgTnnt2.ReaChR∼Citrine.WHVPRE.SV40pA or AAV2/9.45.GgTnnt2.Citrine.WHVPRE.SV40pA diluted with phosphate-buffered saline to a final volume of 700 µL were slowly injected into the tail vein using a 25 G needle (Becton Dickinson, Breda, the Netherlands). Rapamycin (3 mg/kg; LC Laboratories, Woburn, MA) was administered every other day by intraperitoneal injections for 4 weeks. Rats were euthanized by removal of the heart following analgesia with buprenorphine hydrochloride and anaesthesia with isoflurane as described above.

2.3 VT induction and use of multi-LED implant for VT termination *in vivo*

In Week 8–10 post-surgery, animals were anaesthetized as described above and the heart was exposed. VTs were induced by S1S2 programmed electrical stimulation or electrical burst pacing (cycle length 20–30 ms) using a STG4002 stimulus generator with MC Stimulus II software (Multichannel Systems, Reutlingen, Germany). As most self-limited VTs lasted <5 s, optical VT termination was attempted when VTs lasted longer than 5 s. The LED device used in the apical illumination experiments was attached to the apex using two drops of histoacryl tissue glue (B. Braun, Melsungen, Germany). The optical termination protocol consisted of up to three 500 ms pulses with a

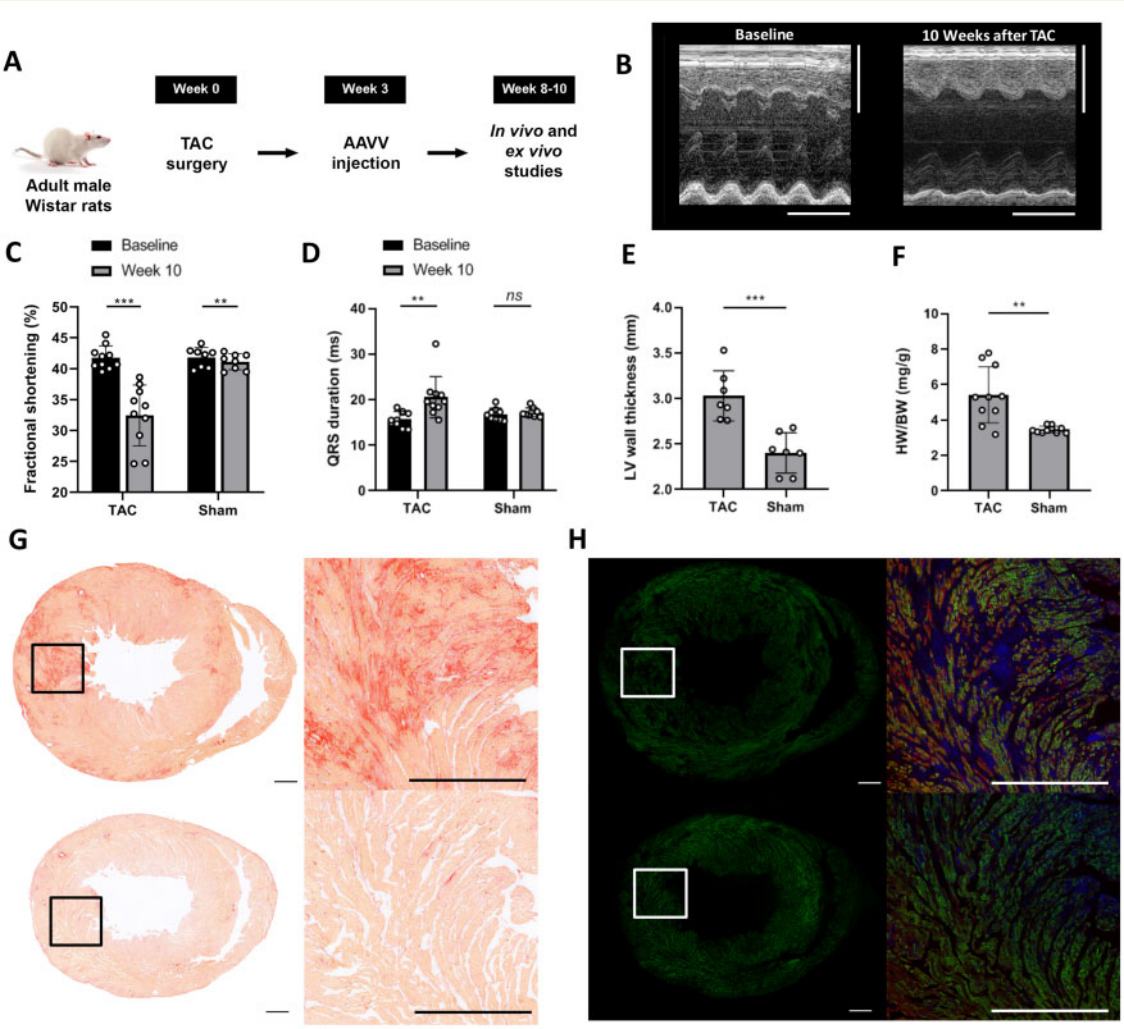

Figure 1 Characterization of the TAC model.
(*A*) Study design. (*B*) Typical example of m-mode echocardiograms showing decreased systolic function at Week 10 after TAC compared to baseline. Vertical scale bars represent 5 mm, the horizontal scale bars represent 250 ms. (*C*) TAC resulted in decreased fractional shortening (***$P \leq 0.001$, **$P = 0.002$ using the paired *t*-test) and (*D*) prolonged QRS duration (*$P = 0.015$ and ns=non-significant using the paired *t*-test) 8–10 weeks after surgery compared to baseline. Each dot represents a single animal, $n=10$ rats per group. (*E*) LV wall thickness (each dot represents a single animal, $n=7$ rats per group) and (*F*) heart weight (mg)-to-body weight (g) ratio (HW/BW) 8–10 weeks after TAC or sham surgery (each dot represents a single animal, $n=10$ rats per group) ***$P \leq 0.001$ using the Student's *t*-test. (*G* and *H*) Representative examples of sirius red (*G*) and immunohistological (*H*) stainings of mid-ventricular transverse sections from one TAC rat (upper pannels) and from one sham-operated rat (lower panels). Sections in (*H*) are immunostained for Citrine (green) and cardiac troponin-I (red). Cell nuclei are stained in blue. The inserts in the left panels of (*G* and *H*) mark the areas depicted in the right panels. Scale bars represent 1 mm.

500 ms interval. The termination protocol was stopped once the VT was terminated. VTs were considered to be optogenetically terminated if the arrhythmia stopped within 1 s following the end of the last light pulse. ECG recordings were acquired and analysed as described earlier.[12]

2.4 Statistics

Statistical analyses were performed using SPSS Statistics v23.0 (IBM, Armonk, NY). The Mann–Whitney *U* test was performed for the comparison of illumination and control groups. Other data were compared by using the two-sided Student's *t*-test for unpaired data and the two-sided paired Student's *t*-test for paired data. Data were expressed as means ± standard deviation or, for arrhythmia termination efficacies, current densities, and membrane potentials as means ± standard error of the mean (SEM). The whole-cell patch clamp measurements are expressed as the means of the raw data; the sharp electrode data are expressed as the means of the means. Differences were considered statistically significant at $P < 0.05$.

3. Results

3.1 Characterization of the TAC model

Evaluation of cardiac contractile and electrophysiological function by echo- and electrocardiography 8–10 weeks after TAC or sham surgery

showed a significantly impaired myocardial fractional shortening (32.5 ± 4.9 vs. 41.8 ± 1.9%, $P \leq 0.001$) and prolonged QRS duration (20.5 ± 4.5 vs. 15.8 ± 1.7 ms, $P = 0.015$) in rats 10 weeks after TAC ($n = 10$). The QRS duration did not significantly change in rats that underwent sham surgery (17.0 ± 1.3 vs. 17.3 ± 0.9 ms, $P = 0.449$ at baseline vs. Week 10, $n = 10$). A significant yet functional irrelevant change was present with regard to the fractional shortening in the sham group (41.1 ± 1.3 vs. 41.8 ± 1.6%, $p = 0.002$ at baseline vs. Week 10) (*Figure 1A–D*). Electrical remodelling in TAC rats was demonstrated by significant prolongation of sharp electrode-derived action potential duration at 80% repolarization (APD_{80}) (97.5 ms vs. 52.3 ms, $P = 0.001$, number of hearts per group: 5, median number of impalements per heart: 2) and ECG-derived corrected QT interval (140 ± 17 vs. 117 ± 5 ms, $P = 0.001$, $n = 10$) when compared to sham-operated animals.

Left ventricular (LV) hypertrophy in TAC rats was demonstrated by a significantly increased LV wall thickness, measured histologically in the mid-papillary short-axis plane (3.03 ± 0.28 vs. 2.40 ± 0.22 mm in sham-operated animals, $P = 0.001$, $n = 7$) (*Figure 1E*), which was in agreement with a significant increased heart-to-body weight ratio (5.3 ± 1.3 mg/g in TAC vs. 3.5 ± 0.2 mg/g in sham-operated rats, $P < 0.001$, $n = 10$) (*Figure 1F*). Further evidence of ventricular remodelling was obtained by histochemical assessment of fibrosis, which demonstrated enhanced deposition of collagen in ventricular myocardium of TAC rats compared to sham-operated controls (5.0 ± 1.6% vs. 1.9 ± 1.6%, $P < 0.001$, $n = 10$) (*Figure 1G*). In addition, the average cell size represented by the whole-cell capacitance of ventricular cardiomyocytes was significantly increased in cells isolated from TAC animals compared to those of sham-operated rats (250 ± 14.3 pF vs. 175 ± 26.3 pF, respectively, $P < 0.05$, $n = 7$), indicating the presence of structural remodelling in TAC hearts at the cellular level.

Intravenous administration of purified ReaChR-encoding AAVV particles (Supplementary material online, *Figure S1A and B*) resulted in similar transduction rates of ventricular cardiomyocytes in TAC and sham-operated rats (71 ± 8% vs. 70 ± 10%, respectively, $P = 0.726$, $n = 10$). Thus, efficient AAVV-mediated optogenetic transgene delivery and expression remained feasible in hearts undergoing pathophysiological changes due to TAC-induced pressure overload (*Figure 1H*).

3.2 Electrophysiological characterization of ReaChR photocurrents and membrane response

Whole-cell patch clamp measurements of ReaChR-expressing ventricular cardiomyocytes showed strong depolarizing photocurrents upon 470 nm illumination (1 s, 10 mW/mm^2) for both TAC and sham-operated rats (*Figure 2A*). This inward current was observed at a wide range of membrane potentials negative to the reversal potential of the ReaChR current (~10 mV) in both groups (*Figure 2B*). Kinetic parameters of the ReaChR current, including time-to-peak and time constant of inactivation and closing were not significantly different between TAC and sham animal-derived cardiomyocytes (*Figure 2C–E*). Illumination at 470 nm produced robust peak (-2.6 ± 0.5 nA vs. -2.5 ± 0.6 nA, $P = 0.9405$) and plateau (-1.4 ± 0.2 nA vs. -1.3 ± 0.3 nA, $P = 0.9479$) photocurrent amplitudes in both the TAC ($n = 8$ cells isolated from five hearts) and sham group ($n = 7$ cardiomyocytes from two hearts), respectively (*Figure 2F and G*). In addition, 470 nm illumination led to sustained plasma membrane depolarization during the entire duration of illumination (*Figure 2H*) from an average resting membrane potential (V_{rest}) of -74.2 ± 0.8 mV and -77.7 ± 3.5 to plateau potentials ($V_{plateau}$) of -15.4 ± 7 mV and -13.5 ± 8.7 mV in cardiomyoctes of TAC ($n = 7$ cells obtained from four hearts) and sham-operated ($n = 5$ cells from two hearts) animals, respectively. There were no statistical differences between the two experimental groups (*Figure 2I and J*), which demonstrates that ReaChR-mediated depolarization of the sarcolemma remains effective in a pathophysiological cardiac substrate.

3.3 Development of a custom-made LED device for apical implantation

Since the penetration depth of visible light increases with its wavelength and ReaChR has a broad action spectrum that extends into the red portion of the visual spectrum,[14] we next performed additional whole-cell patch clamp experiments, sharp electrode measurements, and computational simulations evaluating 470, 567, and 617 nm light in order to find out which wavelengths are the most suited for *in vivo* optogenetic VT termination. Peak photocurrent amplitudes were on average 54.6 ± 8.3% higher for 567 nm and 40 ± 31% higher for 617 nm light pulses when compared to 470 nm light pulses (1 mW/mm^2) ($n = 6$ cardiomyocytes from three hearts, $P = 0.0006$ and $P = 0.0054$, respectively), whereas the plateau photocurrent amplitudes were very similar ($P > 0.05$) across these wavelengths (*Figure 3A and B*). In addition, no significant differences were observed in membrane plateau potentials upon illumination with 500 ms light pulses (1 mW/mm^2) of 470, 567 or 617 nm ($n = 6$ cardiomyocytes from three hearts, $P > 0.05$) (*Figure 3C*). Sharp electrode measurements on ReaChR-expressing apical tissue samples demonstrated strong and sustained membrane depolarization upon illumination with 470, 567, and 617 nm light pulses of 500 ms and with intensities of ≥0.25 mW/mm^2 (*Figure 3D* and Supplementary material online, *Figure S2A*). Importantly, tissue samples were rendered unexcitable for the entire duration of illumination as demonstrated by loss of capture in response to electrical pacing during illumination (from 0.1 mW/mm^2 for 470 and 567 nm light and from 0.25 mW/mm^2 for 617 nm light) (Supplementary material online, *Figure S2B*). However, computer simulations predicted that 567 and 617 nm were more effective in penetrating blood-perfused ventricular myocardium, thus potentially allowing excitation of a substantially larger ventricular mass than can be excited with light of 470 nm (*Figure 3E*). Since these experiments demonstrated that at an intensity of ≥0.25 mW/mm^2, 567 and 617 nm light produced similar membrane potential responses but larger peak photocurrents and improved tissue penetration in comparison to 470 nm light, the 567 nm and 617 nm wavelengths were used for the whole heart experiments. To this end, we designed custom-made 567 and 617 nm multi-LED devices small enough for direct epicardial application *in vivo*. These devices consisted of a central LED surrounded by three equally spaced LEDs with the same specifications (*Figure 4A and B*) and were designed to be attached to the cardiac apex (*Figure 4C and D*) because of its favourable epicardial surface to ventricular mass ratio and central location in relation to both ventricles and septum. In addition, the apex might be an interesting target for optogenetic VT termination since there is evidence that it attracts scroll waves (i.e. re-entrant activity sustaining the arrhythmia) because of its geometrical curvature combined with high levels of anisotropy.[15] Sustained depolarization of the apex might therefore result in highly effective optogenetic VT termination by scroll wave filament destabilization and extinction.

To evaluate the thermal responses of the 567 and 617 nm LED devices when activated for three consecutive 500 ms light pulses with a 500 ms interval, temperature measurements were performed *ex vivo* in an incubator set at 37°C. The maximum temperature of the devices,

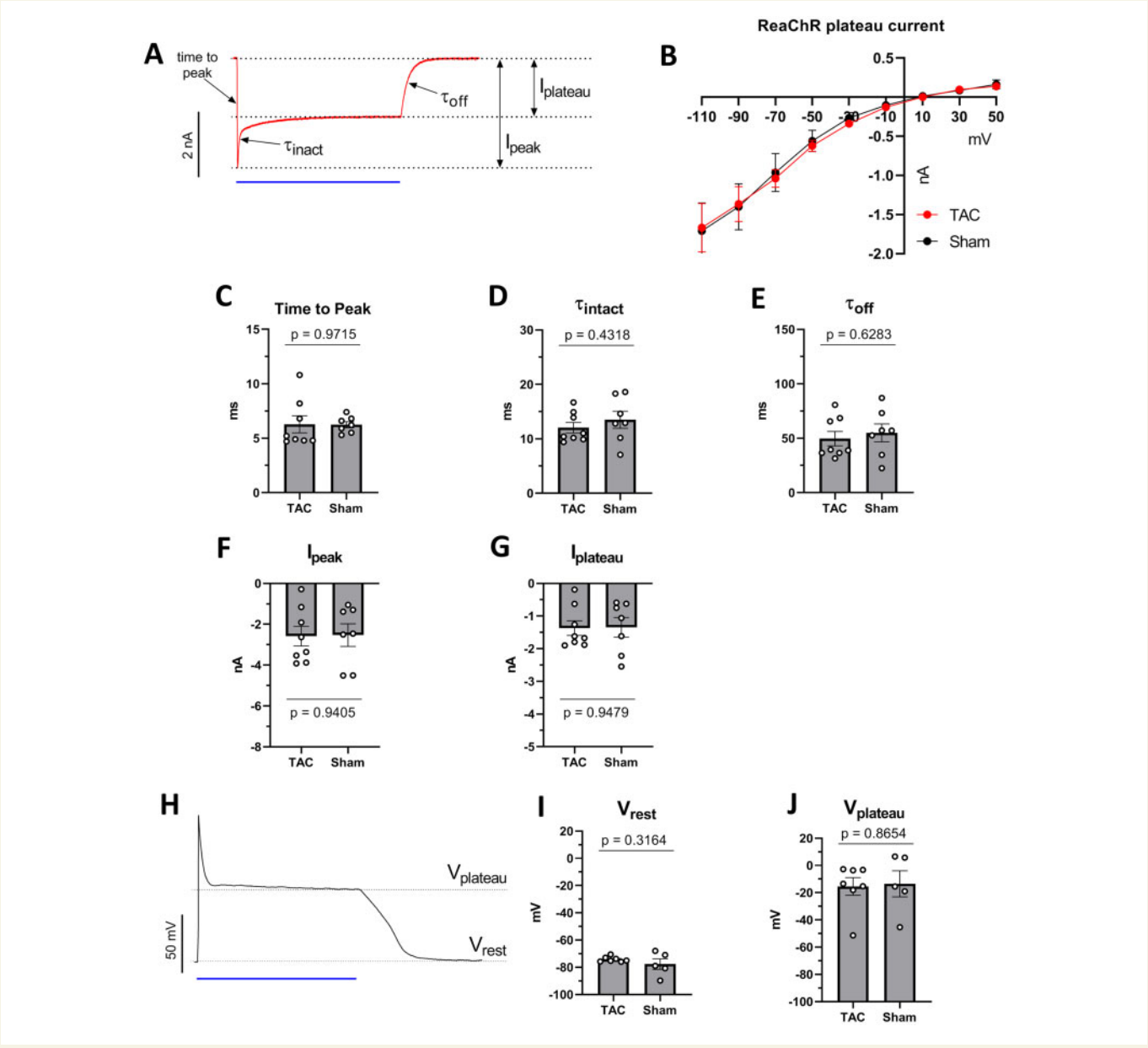

Figure 2 Electrophysiological characterization of ReaChR photocurrents and membrane response in ventricular cardiomyocytes derived from TAC and sham-operated animals.

In all voltage- and current-clamp experiments, ReaChR was activated by 470-nm light (1 s, 10 mW/mm^2). (*A*) Representative whole-cell voltage clamp recording of ReaChR photocurrents from an isolated TAC cardiomyocyte. The membrane potential was clamped at -90 mV. I_{peak}: maximal current amplitude, $I_{plateau}$: current amplitude at the end of the illumination period, time-to-peak: the length of the time interval between the beginning of illumination and the appearance of I_{peak}, τ_{inact}: half-decay time of current decay from I_{peak} to $I_{plateau}$, τ_{off}: half-decay time of current decay from $I_{plateau}$ to zero current. (*B*) ReaChR $I_{plateau}$ amplitudes observed at a range of holding potentials between -110 and 50 mV. (*C*) Time-to-peak values of ReaChR current representing activation kinetics of ReaChR. (*D*) τ_{inact} values of ReaChR current representing ReaChR inactivation kinetics. (*E*) τ_{off} time constant representing ReaChR closing kinetics. (*F* and *G*) ReaChR I_{peak} (*F*) and $I_{plateau}$ (*G*) amplitudes measured at -90 mV holding potentials. (*H*) Representative membrane potential response to 470 nm illumination (blue bar) recorded under current-clamp conditions in a cardiomyocyte isolated from a TAC animal. (*I*) Resting membrane potentials (V_{rest}) observed before illumination. (*J*) Plateau potentials ($V_{plateau}$) measured at the end of the 1 s light pulse. Each dot represents the results of an individual cell. For (*C–H*), $n = 8$ cells from four hearts in the TAC group and $n = 7$ cells from two hearts in the sham group. For (*I*) and (*J*), $n = 7$ cells from four hearts in the TAC group and $n = 5$ cells from two hearts in the sham group. Numerical data are represented as mean ± SEM, all *P*-values were calculated by the Student's *t*-test.

measured on the ventricle-facing surface directly above the PDMS-insulated LED chip, was 36.8°C (range 36.7–37.0°C) before illumination and briefly peaked to an average absolute maximum temperature of 41.1 ± 0.2°C for 567 nm (15 mW/mm^2) and 38.1 ± 0.1°C for 617 nm (10 mW/mm^2) light after the third light pulse (Supplementary material online, *Figure S3A and B*). For the 567 nm LED device, the measured time

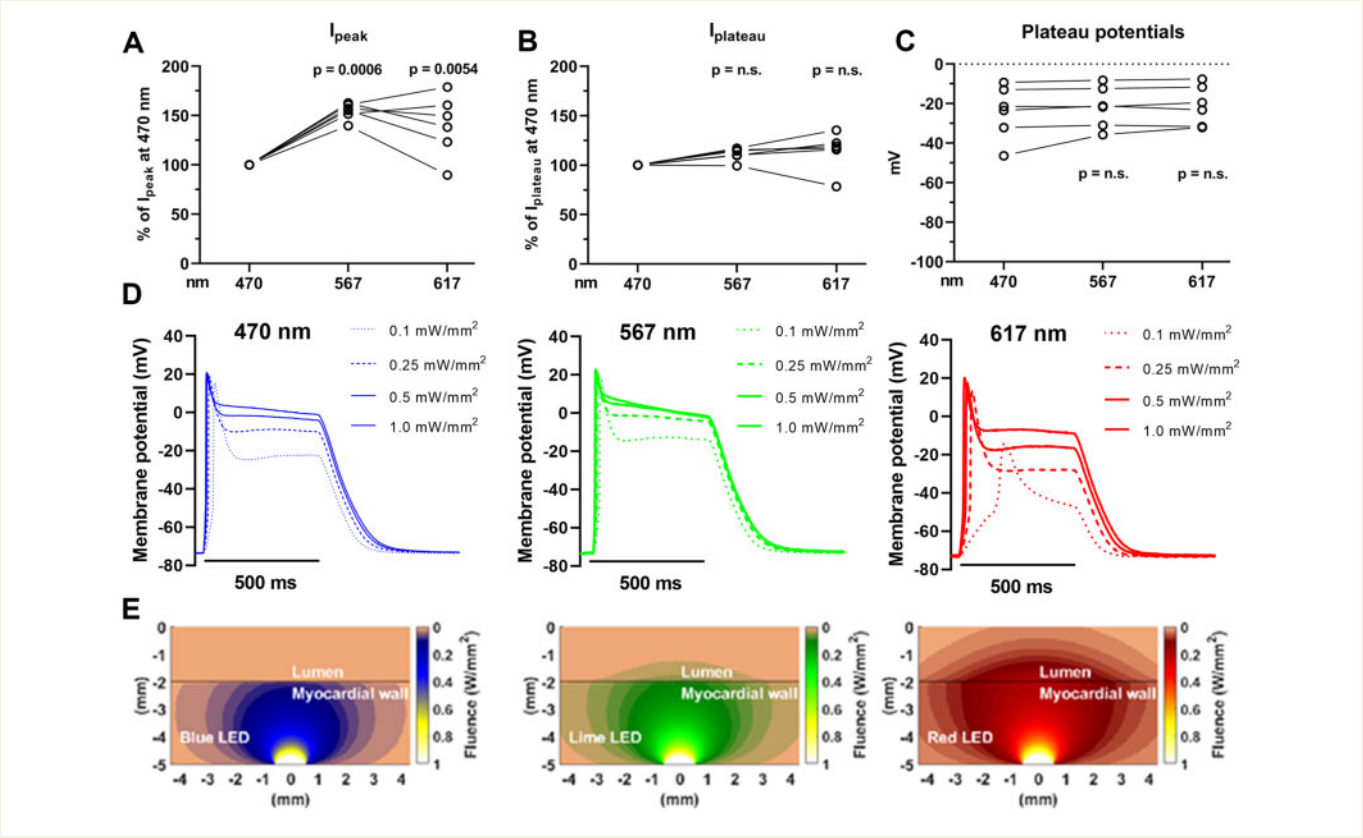

Figure 3 Whole-cell patch clamp and sharp electrode measurements of ReaChR photocurrents and membrane potential responses, and computational light penetration simulations at different excitation wavelengths.
(*A* and *B*) Relative ReaChR I_{peak} (*A*) and $I_{plateau}$ (*B*) amplitudes measured at -90 mV holding potentials upon illumination with 567 or 617 nm light compared to 470 nm light as the index (500 ms, 1 mW/mm^2). Each dot represents the paired results of an individual cell (n=6 cells from four hearts). For the light pulses of 470 nm, the single dots represent averaged values. (*C*) ReaChR plateau potentials ($V_{plateau}$) measured at the end of a 500 ms light pulse (1 mW/mm^2) for 470, 567, and 617 nm light. Each dot represents the results of an individual cell (n=6 cells from four hearts). (*D*) Representative sharp electrode measurements of a ReaChR-expressing ventricular tissue sample from a TAC rat showing sustained depolarization illumination for 500 ms with blue (λ=470 nm), lime (λ=567 nm), or red (λ=617 nm) light of various intensities. All recordings are from the same ventricular spot. (*E*) Computational simulations of propagation of 470, 567, and 617 nm light through rat myocardium.

between 40.0 and 41.1°C was <2 s (Supplementary material online, *Figure S3A*). Importantly, as a safety assessment, optical voltage recordings of the apex after repetitive LED activation *in vivo* and *ex vivo* demonstrated wave front propagation over the entire surface of the apex without regional conduction disturbances, which indicates that attachment and frequent activation of the LED device did not lead to detectable sustained electrophysiological disturbances (*Figure 4E*). This finding is in line with the concept of CEM43 (i.e. cumulative equivalent minutes at 43°C), a standardized thermal dose concept that assesses the impact of different transient heat exposure scenarios on the viability of tissue and cells.[16] In the context of cardiac ablation therapy, it has been proposed that that the critical CEM43 for myocardium is 128 min,[17] well above the CEM43 of <0.1 min in this study.

3.4 Optogenetic VT termination of the remodelled heart by the LED implant *ex vivo*

Each LED device was first evaluated *ex vivo* in isolated TAC hearts using a Langendorff apparatus. After induction of sustained (>10 s) VTs by electrical burst pacing, the LED device was activated for 500 ms up to three times (interval of 500ms) with the LED at the tip of the apex or with all four LEDs covering 1.9 and 7.6 mm^2 of the apical epicardium, respectively. VT termination was feasible with light pulses of 567 and 617 nm (*Figure 5A–C*) in all TAC hearts tested (n = 6). Optogenetic VT termination efficacy after three consecutive 500 ms light pulses (5 mW/mm^2) with the center LED only was 76.7% (SEM 12%) and 60% (SEM 14.6%) using light of 567 and 617 nm, respectively. When all four LEDs were activated, optogenetic VT termination increased to 100% (SEM 0%) for 567 nm and 93.3% (SEM 4.2%) for 617 nm light. VT termination rates in TAC hearts expressing Citrine instead of ReaChR, after three consecutive light pulses with all LEDs activated, were 5% (SEM 5%) and 5% (SEM 5%) for 567 and 617 nm light (n = 4), respectively.

In accordance with the data obtained by sharp electrode measurements, the apex of ReaChR-expressing TAC hearts was rendered refractory upon illumination as demonstrated by a complete loss of capture in response to apical electrical pacing during the entire period of illumination (1000 ms, 5 mW/mm^2) with light of 567 or

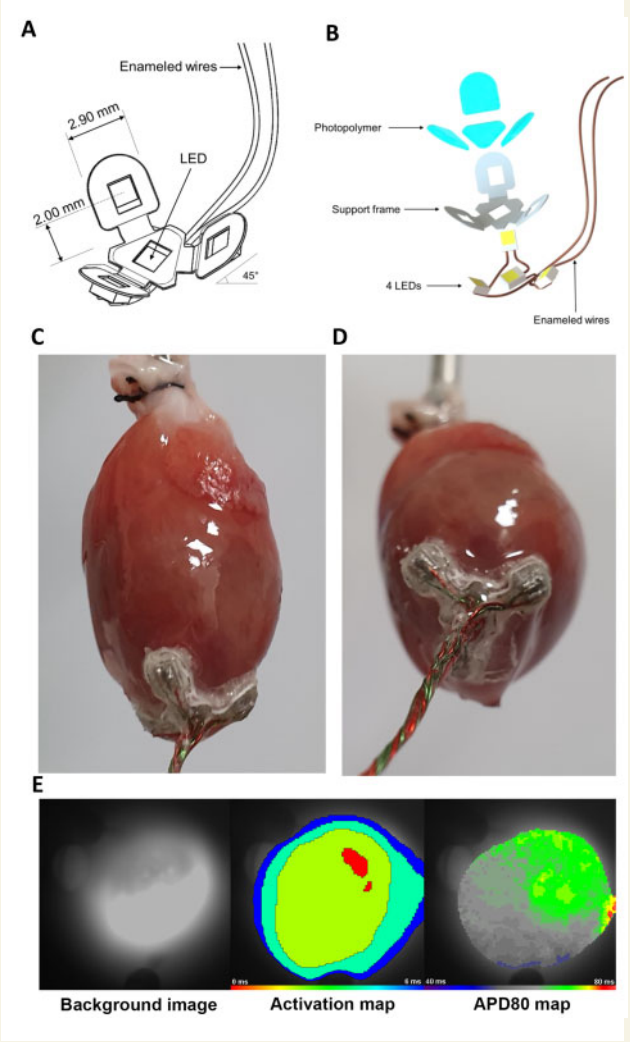

Figure 4 Overview of the apex cup device.
(*A*) Schematic drawing and (*B*) exploded schematic view of the LED assembly. The centrally localized LED chip at the base of the assembly can be activated independently of the other three LEDs. (*C* and *D*) Images of the LED device mounted to the apex of a Langendorff-perfused TAC heart. Firm fixation of the LED device was ensured with tissue adhesive. (*E*) Typical activation (middle panel) and action potential duration at 80% repolarization (APD_{80}, right panel) maps of the apex during sinus rhythm of a ReaChR-expressing TAC heart after it was subjected to repeated LED device activation during *in vivo* and *ex vivo* experiments with all LEDs activated for both 567 nm light (15 mW/mm^2) and 617 nm light (10 mW/mm^2). Recordings were made following LED device removal and with the camera pointed at the tip of the apex (left panel). The activation map demonstrated rapid and regular activation of the epicardial apical surface. The decrease in isochronal line spacing at the edges is due to the curvature of the apex. The APD_{80} map demonstrates a homogenous APD of 60–70 ms.

617 nm ($n = 4$) (*Figure 5D*). As expected, the same illumination conditions did not block apical electrical pacing in Citrine-expressing TAC hearts ($n = 4$) (*Figure 5E*).

3.5 Optogenetic VT termination of the remodelled heart by the LED implant *in vivo*

Next, we evaluated the feasibility and efficacy of optogenetic VT termination by the LED implant *in vivo*. After introduction via the left 6th intercostal space, the LED device was implanted at the apex of anaesthetized and mechanically ventilated TAC rats (*Figure 6A*). Although the thoracic wall could be completely closed with a fully functional LED device *in situ* (*Figure 6A and B*), the optogenetic VT termination experiments were performed with an open incision to facilitate convenient VT induction by programmed electrical stimulation. Following induction of sustained VTs, termination could be realized by one, two, and three 500 ms pulses (*Figure 6C–F* and Supplementary material online, *Figure S4A*). The mean successful optogenetic VT termination rate after three consecutive 500 ms light pulses (567 nm: 15 mW/mm^2; 617 nm: 10 mW/mm^2) was 95% (SEM 5%) for 567 nm light (corresponding to 20 VT episodes in four ReaChR-expressing TAC rats) and 86.7% (SEM 6.7%) for 617 nm light (corresponding to 15 VT episodes in three ReaChR-expressing TAC rats). In Citrine-expressing TAC rats, very few VT episodes terminated under the same illumination conditions (*Figure 6E* and Supplementary material online, *Figure S4B*), resulting in termination rates of 15% (SEM 5%) ($P = 0.015$) and 13.3% (SEM 6.7%) ($P = 0.043$) for light of 567 and 617 nm, respectively (*Figure 6F*). The average RR interval 2 s before VT induction and 2 s after VT termination showed no statistically significant differences for 567 nm (0.252 ± 0.046 vs. 0.260 ± 0.041 s, $n = 18$ individual measurements from four rats; $P = 0.240$) or 617 nm light (0.208 ± 0.017 vs. 0.211 ± 0.022 s, n = 13 individual measurements from three rats; p = 0.514) (*Figure 6G*), i.e. normal rhythm was instantly restored following optical cardioversion.

4. Discussion

Our results demonstrate successful optogenetic VT termination in the structurally and electrically remodelled rat heart *in vivo* by apical illumination using an implanted light source. These results are an important step forward in the clinical development of cardiac optogenetics for ventricular arrhythmia management since the large majority of VT patients exhibit structural heart disease and *in situ* light delivery is an absolute prerequisite for clinical implementation. Previous studies have reported successful optogenetic termination of pharmacologically induced ventricular arrhythmias in explanted, Langendorff-perfused hearts from healthy rodents.[9,11,12,18] In order to mimic structural heart disease characteristics of VT patients, a TAC model was used to induce LV hypertrophy, myocardial fibrosis, reduced cardiac function, and ventricular conduction abnormalities;[19,20] factors that predispose the heart to potentially life-threating arrhythmias. Importantly, we now show that these TAC-induced pathological changes do not impair the transmembrane currents and plateau potentials of ventricular cardiomyocytes and ventricular tissue upon optogenetic modification and subsequent illumination. This substantiated that the prominent anti-arrhythmic mode-of-action of cardiac optogenetics, namely depolarizing photocurrent-induced inhibition of excitation, remains effective under such conditions as demonstrated in our whole heart experiments. In recent studies, Cheng *et al.*[21] found that optogenetic termination of VTs is also feasible during acute ischaemia and chemically induced fibrosis after AAV-mediated channelrhodopsin gene transfer to the hearts of healthy juvenile rats and channelrhodopsin activation by an

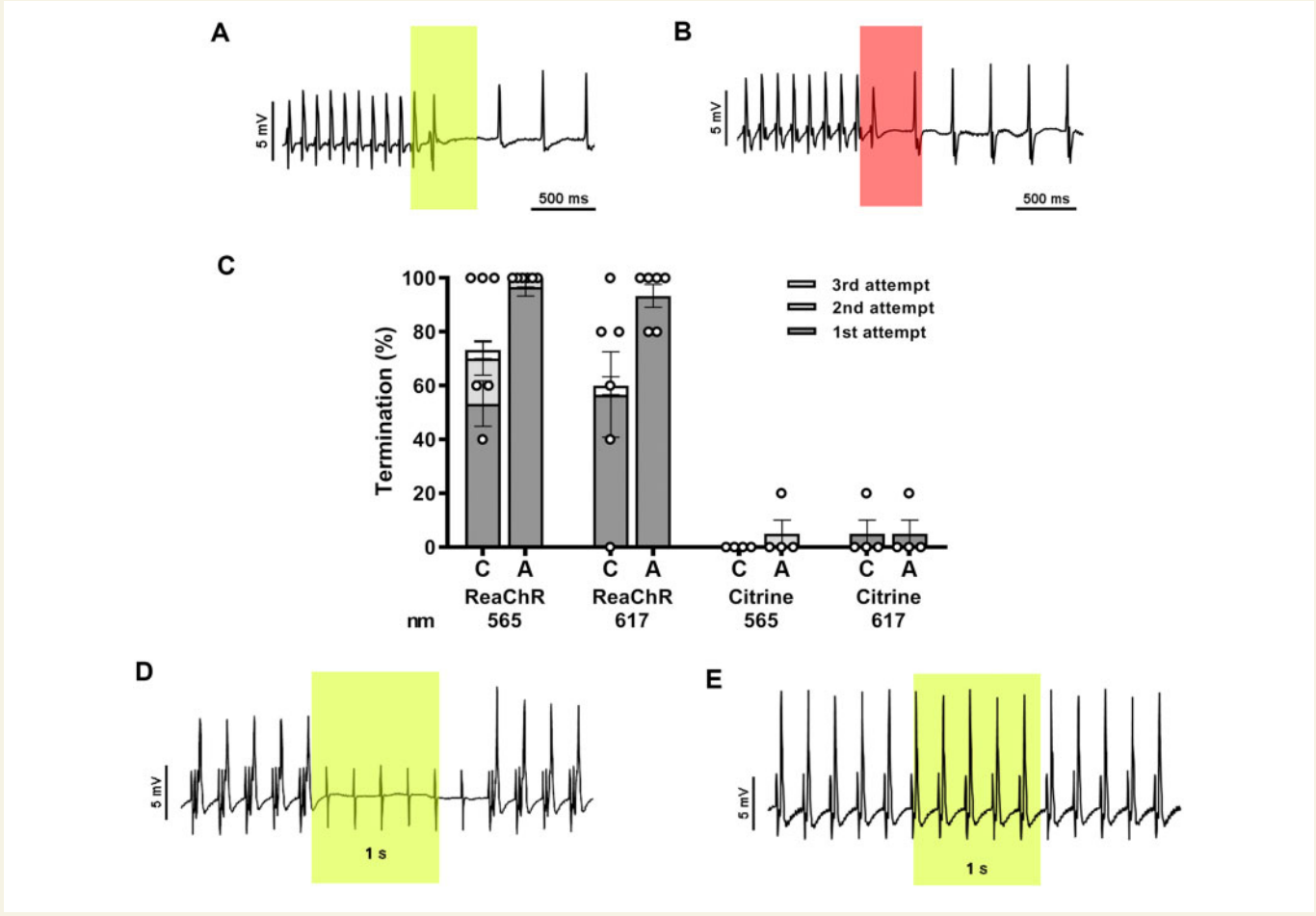

Figure 5 Optogenetic termination of VTs by apical *ex vivo* illumination of TAC hearts with the LED device.
(*A* and *B*) Intracardiac ECG demonstrating successful termination of VTs with a single 567 nm (*A*) or 617 nm (*B*) light pulse (500 ms; 5 mW/mm^2; coloured boxes). (*C*) Quantification of optogenetic termination efficacy averaged per ReaChR-expressing heart (n=6 animals, five individual measurements per animal) or Citrine-expressing heart (n=4 animals, five individual measurements per animal) by the LED device following activation of only the centrally located LED (*C*) or all four LEDs (*A*) for up to three consecutive light pulses (500 ms with a 500 ms cycle length, 5 mW/mm^2). Each dot represents the average of five individual measurements in one rat. Error bars represent SEM. (*D*) Representative intracardiac ECG recording of a ReaChR-expressing TAC heart demonstrating 5 Hz apical pacing before, during, and after apical illumination by the 567 nm LED device with all four LED chips activated for 1000 ms (irradiance: 5 mW/mm^2). The sensing electrode was attached to the LV free wall. Complete loss of ventricular capture during the entire duration of illumination was observed for all ReaChR-expressing TAC animals (n=4) as only pacing artefacts are observed. (*E*) Ventricular capture was not affected by illumination of Citrine-expressing control hearts (n=4).

external blue light source.[22] The use of custom-made implantable light sources emitting red-shifted light allowed us to demonstrate and explain that optical VT termination is feasible in blood-perfused, chronically remodelled hearts *in vivo*. Furthermore, the finding that VT termination can be achieved by illumination of a relatively small area is promising from a clinical perspective.

While this study demonstrated that illumination of larger surface areas increased VT termination rates, it is remarkable that epicardial illumination of ~2 mm^2 of the cardiac apex still resulted in VT termination in most cases. Interestingly, computational studies have suggested that spiral waves driving arrhythmias are more likely to approach the apex of the ventricle rather than the base due to the apex's elliptic shape and high degree of anisotropy.[15] One of the possible underlying mechanisms of local optogenetic VT cardioversion, as demonstrated in this study, might therefore be based on forcing the spiral wave away from the apex towards myocardial regions that favour critical wavefront collisions and subsequent arrhythmia termination. Future dedicated studies are needed to explore this finding in detail as it could lead to more refined optical termination protocols and perhaps a better understanding of anti-arrhythmic mechanisms in general.

Since myocardial light penetration is wavelength-dependent and paramount for effective optogenetic VT termination, we have studied the electrophysiological responses of ReaChR-expressing cells by whole-cell patch clamp experiments and also by sharp electrode measurements on myocardial tissue from TAC hearts. These experiments were complemented with *in silico* studies to simulate light penetration in the rat ventricular wall using a Monte Carlo-based method. The findings of these studies are in agreement with the computational modelling experiments of Karathanos *et al.*[23] showing that optogenetic defibrillation of the human heart was feasible only when red excitation light was used.

Now that the field of optogenetics is maturing into a potential candidate for next generation therapeutics, considerable progress is being made in the development of (i) channelrhodopsins with improved characteristics and (ii) deep *in vivo* light delivery. Such progress includes the

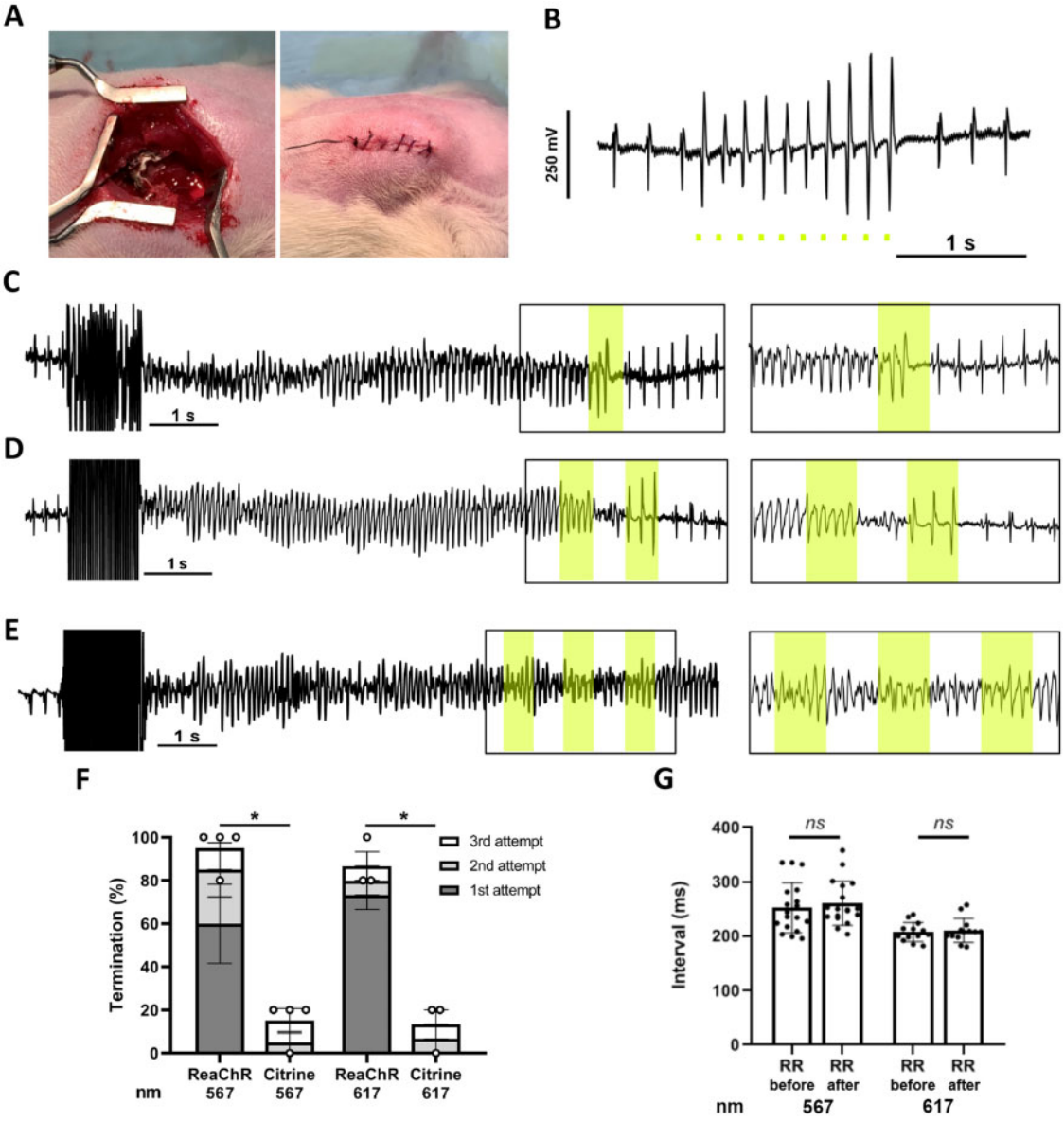

Figure 6 Optogenetic termination of VTs by apical *in vivo* illumination of TAC hearts with the LED device.
(*A*) Picture of LED device implanted at the ventricular apex before and after surgical closure of the thoracic wall, muscle layers, and skin. (*B*) Typical body surface ECG trace showing optical ventricular pacing by the apically implanted LED device with 567 nm light pulses (10 ms; 1 mW/mm^2) under closed-chest conditions. Scale bar represents 1 s. (*C* and *D*) Representative body surface ECG traces showing successful optogenetic termination of VTs by one (*C*) or two (*D*) consecutive 500 ms light pulses (interval: 500 ms) delivered by the 567 nm LED device with all four LEDs activated (irradiance: 15 mW/mm^2; coloured boxes). (*E*) Typical body surface ECG trace showing failure to terminate a VT in a Citrine-expressing control rat by three consecutive light pulses [identical illumination protocol as in (*C*) and (*D*)]. Inserts highlight ECG recordings during illumination. (*F*) Quantification of optogenetic VT termination efficacy *in vivo* averaged per ReaChR- or Citrine-expressing TAC rat (n=4 animals for 567 nm light, n=3 animals for 617 nm light) following activation of all four LEDs by up to three consecutive light pulses (500 ms with a 500 ms cycle length). Irradiance was 15 mW/mm^2 for 567 nm light and 10 mW/mm^2 for 617 nm light. A total of five individual termination attempts were performed per animal. Each dot represents the averaged termination rate of a single animal. Error bars represent SEM. *P <0.05 using the Mann–Whitney U test. (*G*) Graph showing the average RR intervals of the last 2 s before VT induction and the first 2 s after optogenetic VT termination with 567 and 617 nm light pulses. Each dot represents one individual measurement, n =18 measurements from four rats for 567 nm and n=13 measurements from three rats for 617 nm. Data are means. *ns*, non-significant using the paired t-test.

development of channelrhodopsins with enhanced light sensitivity and injectable nanoparticles emitting blue light after excitation with tissue-penetrating near-infrared light,[24–26] which allows optogenetic activation of tissue with large dimensions, e.g. the human-sized heart. In addition, a recent computational study by Hussaini *et al.*[27] demonstrated spiral wave termination in optogenetically modified cardiac tissue by so-called sub-threshold illumination, i.e. by using light intensities too low to evoke an action potential. This finding suggests that smart energy-saving

illumination protocols may suffice to optogenetically terminate cardiac arrhythmic activity under certain conditions. Future *in vivo* studies should reveal which combination of channelrhodopsin, light source and illumination strategy is best suited for termination of a particular type of arrhythmia in a particular pathological substrate. The outcome of such studies could contribute to the design and application of fully implantable optoelectronic devices in favour of optimal efficacy and safety.

In terms of safety, we have measured a maximum temperature at the surface of the LED device of ∼41°C upon consecutive LED activation during thermal response experiments. This value can be considered harmless especially given the very short exposure to this peak temperature. It is important to note that this temperature was measured without the heart attached. Under *in vivo* conditions, the blood-perfused myocardium would act as a biological heatsink, thereby lowering the peak temperature of the LED device. Moreover, optical mapping and sharp electrode experiments of the cardiac apex showed that frequent and repetitive LED exposure during *in vivo* and *ex vivo* experiments did not cause significant abnormalities in wave propagation and electrical excitability. If needed, safety can be further improved by changing the design and materials of the cardiac light sources to reduce the thermal response, which should ideally be explored in future studies in large animal models.

The development of shock-free anti-arrhythmic device treatment for VTs is a much sought-after goal in cardiovascular research and therapy. In the USA alone, a large and growing number of ICDs are implanted annually to protect patients from potentially life-threatening VTs. While these devices have shown to improve survival in different subsets of patients, they are also known to cause long-lasting adverse effects on quality of life among those who have experienced shocks, especially when delivered inappropriately.[6] Shock-free cardioversion of VTs, as potentially provided by cardiac optogenetics, may overcome the adverse effects of conventional ICDs as it would render the use of electric shocks for VT termination obsolete. This could not only increase the quality of life of ICD patients, but potentially even improve the prognosis as ICD shocks can cause direct myocardial injury.[28]

Several important steps have to be taken before optogenetic cardioversion therapy for VTs can be clinically studied. In essence, two important components need to be in place in order to enable optogenetic arrhythmia termination, namely (i) sufficiently high and widespread expression of opsins in the myocardium and (ii) activation of these opsins by adequate cardiac light delivery. While widespread cardiac transgene expression in large animal studies and human clinical trials is difficult to achieve, robust local transgene expression could be obtained by gene delivery methods, such as epicardial gene painting or by intramyocardial injections.[29,30] For example, in this study, ReaChR was expressed throughout the heart due to the systemic administration of AAVVs, however only a small portion of the heart was illuminated by the implanted LED device. This important finding suggests that merely targeting the cardiac apex, e.g. by multiple intramyocardial injections,[31] might be sufficient to create the optogenetic substrate that is needed for shock-free cardioversion. Local illumination of the cardiac apex may be realized by ultrathin, biocompatible, and flexible LED-sheets[32,33] inserted via minimal invasive thoracic surgery or by percutaneous light fibre implantation into the myocardium.[34] The latter approach has the advantage that all light is directly delivered to the myocardial wall, thereby maximizing illumination efficiency. In addition, when inserted mid-myocardially, the maximum distance between the light source and the opposite myocardial boundaries is minimized resulting in maximal light exposure of the ventricular wall. Future studies in larger animal models should focus on the potential short- and long-term effects of epicardial LED implantation, especially on mechanical function. Possible impairment of contractile activity could be overcome by the development of devices specifically designed for cardiac optogenetic purposes that take cardiac mechanical properties into account.[33,35,36] For these thin, stretchable, and biocompatible devices, the best suited anatomical site for implantation within the thorax should be identified through rigorous investigation focusing on the optimal efficacy and safety of this intervention.

In our study, the cardiac substrate for VT was a hypertrophic cardiomyopathy model exhibiting signs of structural and electrical remodelling. Although this model has been a solid starting point for evaluating optogenetic VT termination in the remodelled heart by an implantable LED device and local optogenetic targeting, from a translational perspective, it will be important to evaluate the applicability of this approach in other cardiac diseases as well, for example by applying (i) models of acute ischaemia, (ii) chronic infarction models with scar formation, and (iii) heart failure models not based on chronic pressure overload caused by TAC. Furthermore, since the computational light penetration simulations in our study did not take account for the (small) light sensitivity differences of ReaChR per wavelength, future studies are needed to determine the cardiac mass that is effectively excited upon optogenetic illumination by different-coloured light and how this relates to efficacy of optogenetic VT termination. In addition, since this study made use of male animals, future studies should also include female animals in order to investigate potential gender differences.

In summary, although more translational studies are required, our findings do provide important new insights into the translational potential of pain-free cardioversion therapy by optogenetics. This was done by demonstrating this approach in a pathologically relevant *in vivo* model of VT through implant-based local red-shifted light delivery.

Supplementary material

Supplementary material is available at *Cardiovascular Research* online.

Authors' contributions

E.C.A.N., A.A.F.d.V., and D.A.P. conceived the study, interpreted results, and wrote the manuscript. E.C.A.N., M.S.F., T.v.d.H., and V.P. performed animal experiments and statistical analysis. T.J.v.B., C.R., G.Q.Z., and R.H.P. designed and fabricated the LED device and performed the optical modelling studies. B.O. performed the whole-cell path clamp and sharp electrode measurements. C.I.B. and A.A.F.d.V. designed and produced AAVVs. K.Z., M.J.S., T.J.v.B., and A.A.R. helped in interpreting the data. All authors refined the manuscript.

Acknowledgements

We would like to thank Roman Koning and Ronald Limpens (Department of Cell and Chemical Biology, LUMC) for producing the electron microscopic images and Minka Bax (Department of Cardiology, LUMC) for excellent assistance during animal experiments.

Funding

This study was supported by European Research Council (Starting grant 716509 to D.A.P.). Additional support was provided by the Netherlands Organization for Scientific Research (Vidi grant 91714336 to D.A.P.).

Conflict of interest: none declared.

Data availability

The data underlying this article are available in the article and in its Supplementary material online.

References

1. Al-Khatib SM, Stevenson WG, Ackerman MJ, Bryant WJ, Callans DJ, Curtis AB, Deal BJ, Dickfeld T, Field ME, Fonarow GC, Gillis AM, Granger CB, Hammill SC, Hlatky MA, Joglar JA, Kay GN, Matlock DD, Myerburg RJ, Page RL. 2017 AHA/ACC/HRS guideline for management of patients with ventricular arrhythmias and the prevention of sudden cardiac death: executive summary: A Report of the American College of Cardiology/American Heart Association Task Force on Clinical Practice Guidelines and the Heart Rhythm Society. *Heart Rhythm* 2018;**15**:e190–e252.
2. John RM, Tedrow UB, Koplan BA, Albert CM, Epstein LM, Sweeney MO, Miller AL, Michaud GF, Stevenson WG. Ventricular arrhythmias and sudden cardiac death. *Lancet* 2012;**380**:1520–1529.
3. Roberts-Thomson KC, Lau DH, Sanders P. The diagnosis and management of ventricular arrhythmias. *Nat Rev Cardiol* 2011;**8**:311–321.
4. Bradfield JS, Ajijola OA, Vaseghi M, Shivkumar K. Mechanisms and management of refractory ventricular arrhythmias in the age of autonomic modulation. *Heart Rhythm* 2018;**15**:1252–1260.
5. Josephson M, Wellens HJ. Implantable defibrillators and sudden cardiac death. *Circulation* 2004;**109**:2685–2691.
6. Magyar-Russell G, Thombs BD, Cai JX, Baveja T, Kuhl EA, Singh PP, Montenegro Braga Barroso M, Arthurs E, Roseman M, Amin N, Marine JE, Ziegelstein RC. The prevalence of anxiety and depression in adults with implantable cardioverter defibrillators: a systematic review. *J Psychosom Res* 2011;**71**:223–231.
7. Deisseroth K. Optogenetics. *Nat Methods* 2011;**8**:26–29.
8. Nussinovitch U, Gepstein L. Optogenetics for in vivo cardiac pacing and resynchronization therapies. *Nat Biotechnol* 2015;**33**:750–754.
9. Bruegmann T, Boyle PM, Vogt CC, Karathanos TV, Arevalo HJ, Fleischmann BK, Trayanova NA, Sasse P. Optogenetic defibrillation terminates ventricular arrhythmia in mouse hearts and human simulations. *J Clin Invest* 2016;**126**:3894–3904.
10. Vogt CC, Bruegmann T, Malan D, Ottersbach A, Roell W, Fleischmann BK, Sasse P. Systemic gene transfer enables optogenetic pacing of mouse hearts. *Cardiovasc Res* 2015;**106**:338–343.
11. Crocini C, Ferrantini C, Coppini R, Scardigli M, Yan P, Loew LM, Smith G, Cerbai E, Poggesi C, Pavone FS, Sacconi L. Optogenetics design of mechanistically-based stimulation patterns for cardiac defibrillation. *Sci Rep* 2016;**6**:35628.
12. Nyns ECA, Kip A, Bart CI, Plomp JJ, Zeppenfeld K, Schalij MJ, de Vries AAF, Pijnappels DA. Optogenetic termination of ventricular arrhythmias in the whole heart: towards biological cardiac rhythm management. *Eur Heart J* 2017;**38**:2132–2136.
13. Del Monte F, Butler K, Boecker W, Gwathmey JK, Hajjar RJ. Novel technique of aortic banding followed by gene transfer during hypertrophy and heart failure. *Physiol Genomics* 2002;**9**:49–56.
14. Lin JY, Knutsen PM, Muller A, Kleinfeld D, Tsien RY. ReaChR: a red-shifted variant of channelrhodopsin enables deep transcranial optogenetic excitation. *Nat Neurosci* 2013;**16**:1499–1508.
15. Pravdin S, Dierckx H, Markhasin VS, Panfilov AV. Drift of scroll wave filaments in an anisotropic model of the left ventricle of the human heart. *Biomed Res Int* 2015;**2015**:389830.
16. Sapareto SA, Dewey WC. Thermal dose determination in cancer therapy. *Int J Radiat Oncol Biol Phys* 1984;**10**:787–800.
17. Tian Z, Nan Q, Nie X, Dong T, Wang R. The comparison of lesion outline and temperature field determined by different ways in atrial radiofrequency ablation. *Biomed Eng Online* 2016;**15**:124.
18. Quinonez Uribe RA, Luther S, Diaz-Maue L, Richter C. Energy-reduced arrhythmia termination using global photostimulation in optogenetic murine hearts. *Front Physiol* 2018;**9**:1651.
19. deAlmeida AC, van Oort RJ, Wehrens XH. Transverse aortic constriction in mice. *J Vis Exp* 2010;**38**:1729.
20. Xia Y, Lee K, Li N, Corbett D, Mendoza L, Frangogiannis NG. Characterization of the inflammatory and fibrotic response in a mouse model of cardiac pressure overload. *Histochem Cell Biol* 2009;**131**:471–481.
21. Cheng Y, Li H, Wang L, Li J, Kang W, Rao P, Zhou F, Wang X, Huang C. Optogenetic approaches for termination of ventricular tachyarrhythmias after myocardial infarction in rats in vivo. *J Biophotonics* 2020;**13**:e202000003.
22. Li J, Wang L, Luo J, Li H, Rao P, Cheng Y, Wang X, Huang C. Optical capture and defibrillation in rats with monocrotaline-induced myocardial fibrosis 1 year after a single intravenous injection of adeno-associated virus channelrhodopsin-2. *Heart Rhythm* 2020;**18**:109–117.
23. Karathanos TV, Bayer JD, Wang D, Boyle PM, Trayanova NA. Opsin spectral sensitivity determines the effectiveness of optogenetic termination of ventricular fibrillation in the human heart: a simulation study. *J Physiol* 2016;**594**:6879–6891.
24. Rajasethupathy P, Sankaran S, Marshel JH, Kim CK, Ferenczi E, Lee SY, Berndt A, Ramakrishnan C, Jaffe A, Lo M, Liston C, Deisseroth K. Projections from neocortex mediate top-down control of memory retrieval. *Nature* 2015;**526**:653–659.
25. Chen S, Weitemier AZ, Zeng X, He L, Wang X, Tao Y, Huang AJY, Hashimotodani Y, Kano M, Iwasaki H, Parajuli LK, Okabe S, Teh DBL, All AH, Tsutsui-Kimura I, Tanaka KF, Liu X, McHugh TJ. Near-infrared deep brain stimulation via upconversion nanoparticle-mediated optogenetics. *Science* 2018;**359**:679–684.
26. Kim S, Kyung T, Chung JH, Kim N, Keum S, Lee J, Park H, Kim HM, Lee S, Shin HS, Do Heo W. Non-invasive optical control of endogenous Ca(2+) channels in awake mice. *Nat Commun* 2020;**11**:210.
27. Hussaini S, Venkatesan V, Biasci V, Romero Sepulveda JM, Quinonez Uribe RA, Sacconi L, Bub G, Richter C, Krinski V, Parlitz U, Majumder R, Luther S. Drift and termination of spiral waves in optogenetically modified cardiac tissue at sub-threshold illumination. *Elife* 2021;**10**:e59954.
28. Sham'a RA, Nery P, Sadek M, Yung D, Redpath C, Perrin M, Sarak B, Birnie D. Myocardial injury secondary to ICD shocks: insights from patients with lead fracture. *Pacing Clin Electrophysiol* 2014;**37**:237–241.
29. Kikuchi K, McDonald AD, Sasano T, Donahue JK. Targeted modification of atrial electrophysiology by homogeneous transmural atrial gene transfer. *Circulation* 2005;**111**:264–270.
30. Liu Z, Hutt JA, Rajeshkumar B, Azuma Y, Duan KL, Donahue JK. Preclinical efficacy and safety of KCNH2-G628S gene therapy for postoperative atrial fibrillation. *J Thorac Cardiovasc Surg* 2017;**154**:1644–1651.e1648.
31. Gabisonia K, Prosdocimo G, Aquaro GD, Carlucci L, Zentilin L, Secco I, Ali H, Braga L, Gorgodze N, Bernini F, Burchielli S, Collesi C, Zandona L, Sinagra G, Piacenti M, Zacchigna S, Bussani R, Recchia FA, Giacca M. MicroRNA therapy stimulates uncontrolled cardiac repair after myocardial infarction in pigs. *Nature* 2019;**569**:418–422.
32. Kim RH, Kim DH, Xiao J, Kim BH, Park SI, Panilaitis B, Ghaffari R, Yao J, Li M, Liu Z, Malyarchuk V, Kim DG, Le AP, Nuzzo RG, Kaplan DL, Omenetto FG, Huang Y, Kang Z, Rogers JA. Waterproof AlInGaP optoelectronics on stretchable substrates with applications in biomedicine and robotics. *Nat Mater* 2010;**9**:929–937.
33. Park SI, Brenner DS, Shin G, Morgan CD, Copits BA, Chung HU, Pullen MY, Noh KN, Davidson S, Oh SJ, Yoon J, Jang KI, Samineni VK, Norman M, Grajales-Reyes JG, Vogt SK, Sundaram SS, Wilson KM, Ha JS, Xu R, Pan T, Kim TI, Huang Y, Montana MC, Golden JP, Bruchas MR, Gereau RWt, Rogers JA. Soft, stretchable, fully implantable miniaturized optoelectronic systems for wireless optogenetics. *Nat Biotechnol* 2015;**33**:1280–1286.
34. Zgierski-Johnston CM, Ayub S, Fernandez MC, Rog-Zielinska EA, Barz F, Paul O, Kohl P, Ruther P. Cardiac pacing using transmural multi-LED probes in channelrhodopsin-expressing mouse hearts. *Prog Biophys Mol Biol* 2020;**154**:51–61.
35. Xu L, Gutbrod SR, Ma Y, Petrossians A, Liu Y, Webb RC, Fan JA, Yang Z, Xu R, Whalen JJ III, Weiland JD, Huang Y, Efimov IR, Rogers JA. Materials and fractal designs for 3D multifunctional integumentary membranes with capabilities in cardiac electrotherapy. *Adv Mater* 2015;**27**:1731–1737.
36. Fang H, Zhao J, Yu KJ, Song E, Farimani AB, Chiang CH, Jin X, Xue Y, Xu D, Du W, Seo KJ, Zhong Y, Yang Z, Won SM, Fang G, Choi SW, Chaudhuri S, Huang Y, Alam MA, Viventi J, Aluru NR, Rogers JA. Ultrathin, transferred layers of thermally grown silicon dioxide as biofluid barriers for biointegrated flexible electronic systems. *Proc Natl Acad Sci USA* 2016;**113**:11682–11687.

Translational perspective

Ventricular tachyarrhythmias (VTs) often require delivery of electric shocks for acute restoration of sinus rhythm. These high-voltage shocks are, however, not only causing depression and tissue damage, but may also be delivered inappropriately. A fully shock-free approach can be realized via optogenetics by allowing optical cardioversion. This study adds to the perspective of optical rhythm restoration by addressing various key translational aspects of this novel strategy to reveal that apical illumination of the pathologically remodelled heart *in vivo*, by a custom-made implanted multi-LED device, results in robust and safe VT termination in the intact adult rat upon cardiac optogenetic modification.